

# THEMIS Na exosphere observations of Mercury and their correlation with *in-situ* magnetic field measurements by MESSENGER

V. Mangano (1), S. Massetti (1), A. Milillo (1), C. Plainaki (1), S. Orsini (1), R. Rispoli (1) and F. Leblanc (2)

(1) INAF/IAPS, Roma, Italy (2) LATMOS/IPSL, Paris, France  
 (valeria.mangano@iaps.inaf.it)

## Abstract

The Na exosphere of Mercury is being studied since its discovery in mid '80s from Earth-based telescopes, and it has revealed a high dynamics and variability. Although the processes and their relationships characterising the Hermean exosphere generation and dynamics are still not exhaustively understood, there are no doubts on a tight interconnection among the planet's surface, exosphere, intrinsic magnetic field, the Solar Wind and the Interplanetary Magnetic Field (IMF). Here we analyse an extended dataset of images of the exospheric Na emission, collected from 2009 to 2013, by means of the THEMIS ground-based telescope, and perform a comprehensive statistical study of the recurrent Na emission patterns, and also their potential relationship with the IMF variability. For this purpose, we take advantage of a subset (years 2011-2013) of contemporary *in situ* measurements of the IMF obtained by the MAG instrument on-board the MESSENGER spacecraft.

symmetrical (with respect to equator) single peak pattern EP (9.3%) and unsymmetrical single peak patterns EPN (6.9%) and EPS (6.1%) occur in 84 cases (22.3%). The WP is about twice as frequent as EP (16.4%). The remaining 61.3% of cases belongs to double peaks patterns: 45 cases of 2P (11.9%), 45 of 2PC (11.9%), 80 cases of 2PN (21.2%) and 61 of 2PS (16.2%). These data confirms that, on the long term, the double peak emission is the most frequent Na exospheric configuration. On the other hand, the most frequent exospheric Na emission pattern is a different one each year, that is: 2P in 2009, 2PS in 2010, 2PN in 2012 and in 2013. The 2011 only shows a predominance of the single peak patterns (EP and WP).

## 1. THEMIS data: recurrent patterns

A wide database of 644 images obtained from yearly observations of Mercury by the THEMIS solar telescope in Tenerife is analyzed to identify the recurrent Na emission patterns for years 2009-2013. They can be mainly divided into two categories: single peak centered on the sub-solar point, or two symmetric peaks at high/mid latitude position along noon meridian. Inside each of the two categories, we can further divide the different morphologies into 8 different types (see Figure 1). Final unbiased statistical analysis of the 377 'good' images are summarized in Table 1 where the images are also divided according to the geometry of observation (East or West longitude). Table 1 shows that the

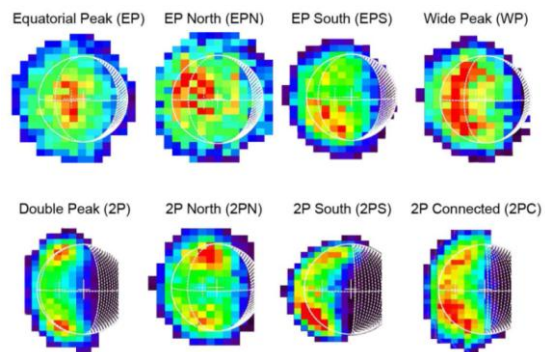


Figure 1: The 8 recurrent Na emission patterns.

Table 1: List of the 8 different exospheric patterns.

TYPE OF PATTERN	2009		2010		2011		2012		2013		5 years		total	
	east	west tot	east	west tot	east	west tot	east	west tot	east	west tot	east	west tot		
Equatorial peak	7	7	4	4	12	10	22	1	1	1	14	21	35	
E. Peak North			2	2	3	3	15	15	6	6	23	3	26	
E. Peak South	6	6	12	12	4	4			1	1	23	23	84	
Wide peak	7	7	7	5	12	1	26	27	9	9	7	24	88	
2 Peaks	25	8	33	3	3	2	2	5	5	2	2	32	13	45
2 Peaks Connected	3	7	10	3	7	10	5	5	15	15	5	26	19	40
2 Peaks North +	27	1	28	2	4	6	2	2	30	30	14	14	73	80
2 Peaks South +	4	11	15	32	32	7	7	1	1	1	5	6	6	61
TOTAL		106		81		72		76		42		377	644	
Rejected		82		49		29		13		94		267		

## 2. THEMIS data: full-disk analysis

In addition, we use a subset of images (79) taken when most of the illuminated disk was in view ( $\geq 90\%$ ) to account for the possible reasons of these symmetries, and to analyse whether asymmetries occur also in longitude. A summary is given in Table 2. We analysed the position of the Na emission patterns (both single and double peak) with respect to the sub-solar meridian (noon) and subdivided them into three regions: *pre-noon*, *noon* and *post-noon*, accordingly to the location of the patterns (see Figure 2), and found that they are mostly located in the pre-noon (53%) and noon (35%) regions (see Table 2). A check on the East or West elongation occurring during the observation shows that the subset of images is equally distributed between Eastern and Western elongations, hence minimizing possible systematic errors due to visual geometry. In addition, we also find that the Double Peak patterns observed in this set of *quasi-full disk* images are all roughly located along the same meridian, i.e. no longitudinal shift of one peak with respect to the other is clearly evidenced.

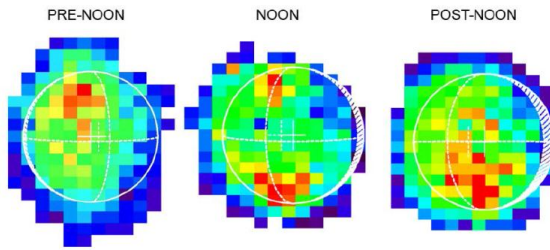


Figure 2: Examples of the pre-noon, noon and post-noon Na emission patterns.

Table 2: List of the 8 different exospheric patterns in the sub-set of 90% visibility of the disk.

TYPE OF PATTERN	2009			2011			2012			2013			5 years			Total
	pre	noon	post	pre	noon	post	pre	noon	post	pre	noon	post	pre	noon	post	
Equatorial peak	3	2											4	2		27
E. Peak North				2	1	11							11	3	1	3
E. Peak South	4	1								1			4	1		3
Wide peak	4	1				2	3	1					7	2		11
2 Peaks				1											3	3
2 Peaks Connected	5	1		2		4	1	1					9	3	1	41
2 Peaks North +	3	4			1	2	5	2		1	4	2	3	3	5	5
2 Peaks South +													4	8		5
TOTAL	19	9	0	0	5	4	21	8	3	2	5	3	42	28	9	79

## 3. MAG data & correlation with THEMIS

Depending on the spacecraft position along the orbit, the MAG sensor collects data from both the IMF or the magnetosphere of Mercury (Figure 3). MESSENGER was orbiting around Mercury since

March 2011. Hence, since that moment contemporary data of global exospheric Na mapping and in-situ measurements of the IMF B-field are available (years 2011-2013). We calculated the occurrence of the different patterns for each IMF component, by subdividing the magnetic field strength and sign into four ranges:  $B_i \geq 10$  nT,  $10$  nT  $\geq B_i \geq 0$  (strongly and moderately positive),  $0 \geq B_i \geq -10$  nT,  $-10$  nT  $\geq B_i$  (moderately and strongly negative). Table 3 summarizes the results (NB. Note that we have only 1 2PS event occurring in the present analysis and it was omitted from the statistics). The stronger correlation between IMF and Na emission patterns occurs for the double peak set, where IMF  $B_x$  is mainly  $> 0$ , and IMF  $B_y < 0$ . The IMF  $B_z$  is strongly negative in the 2P case. On the contrary, the single peak set shows less definite correlation: IMF  $B_x$  ranges from strongly positive to strongly negative, in EP and WP configurations, respectively. The IMF  $B_z$  is mostly negative in EP patterns (58%), while is positive in 53% of WP ones.

		SINGLE PEAK							
		$B_x$	$B_y$	$B_z$	$B_x$	$B_y$	$B_z$		
ALL	$B \geq 10$	39%	34%	9%	37%	37%	14%		
	$0 < B < 10$	6%	30%	40%	3%	23%	40%		
	$-10 < B < 0$	6%	21%	36%	11%	20%	23%		
	$B \leq -10$	49%	15%	15%	49%	20%	23%		
EP	$B \geq 10$	75%	8%	17%	67%	13%	21%		
	$0 < B < 10$	8%	25%	25%	0%	27%	53%		
	$-10 < B < 0$	0%	42%	50%	6%	33%	13%		
	$B \leq -10$	17%	25%	8%	27%	27%	13%		
WP	$B \geq 10$	21%	42%	0%	17%	50%	11%		
	$0 < B < 10$	5%	37%	53%	5%	22%	33%		
	$-10 < B < 0$	5%	10%	31%	17%	11%	28%		
	$B \leq -10$	69%	11%	16%	61%	17%	28%		

THEMIS - MAG (-1 h)

THEMIS - MAG



		DOUBLE PEAK							
		$B_x$	$B_y$	$B_z$	$B_x$	$B_y$	$B_z$		
ALL	$B \geq 10$	71%	17%	12%	70%	19%	16%		
	$0 < B < 10$	0%	17%	37%	0%	21%	33%		
	$-10 < B < 0$	3%	20%	37%	2%	9%	35%		
	$B \leq -10$	26%	46%	14%	28%	51%	16%		
2P	$B \geq 10$	72%	14%	13%	88%	13%	12%		
	$0 < B < 10$	0%	29%	29%	0%	12%	12%		
	$-10 < B < 0$	14%	14%	29%	0%	12%	13%		
	$B \leq -10$	14%	43%	29%	12%	63%	63%		
2PC	$B \geq 10$	73%	18%	19%	57%	29%	14%		
	$0 < B < 10$	0%	19%	27%	0%	21%	36%		
	$-10 < B < 0$	0%	27%	27%	0%	7%	43%		
	$B \leq -10$	27%	36%	27%	43%	43%	7%		
2PN	$B \geq 10$	69%	19%	6%	70%	15%	15%		
	$0 < B < 10$	0%	12%	50%	0%	25%	40%		
	$-10 < B < 0$	0%	13%	44%	5%	10%	40%		
	$B \leq -10$	31%	56%	0%	25%	50%	5%		

THEMIS - MAG (-1 h)

THEMIS - MAG

Table 3: Statistics of the IMF  $B_X$ ,  $B_Y$  and  $B_Z$  1-h averages. On the top/bottom the results obtained in the case of for the single/double peak patterns. The right columns show the IMF averages computed on the same time period of the Na measurements (THEMIS-MAG), the left ones show the IMF averages calculated 1-hour ahead the observations (THEMIS-MAG (-1 h)). Darker cells and bold digits indicate higher occurrence rates (see legend). Cells marked with thick borders indicate the most significant IMF  $B_Z$  values.

## 4. Conclusions

We performed a statistical analysis of the Na emission from the exosphere of Mercury, based on ground based observations taken by the THEMIS telescope, and spanning over a time period of 5 years (2009-2013). We categorized the exospheric Na emission into 8 different recurrent patterns and studied their occurrence rate, also as a function of the in situ IMF, as measured by the MAG instrument on-board the MESSENGER spacecraft. The results of this study can be summarized as follows:

1. by considering the whole THEMIS database, we found that the equatorial peak patterns and the high latitude double peak patterns are mutually exclusive. The latter being the most common (61%) Na emission feature, often observed continuously for several hours: this supports the idea that the solar wind ion precipitation through the polar cusps has a crucial role in the generation of the observed high latitude Na exospheric emission;
2. on average, the observed double peak patterns do not show a statistically significant North-South asymmetry: if these are actually connected to the ion precipitation into the polar cusps, this fact favours the idea that the Mercury's magnetic dipole is symmetrical with respect to the equatorial plane, and also implies that the role of the IMF  $B_X$  in driving the magnetic reconnection in the Hermean magnetosphere is weaker than foreseen;
3. the analysis of the exospheric Na emission pattern as a function of the IMF, even if preliminary (due to the difficulty to have simultaneous in-situ IMF data), shows that the high latitude double peak pattern (2P) is more frequently observed during negative IMF  $B_Z$  periods (76%), whereas the single equatorial peak emission (EP) is more common when the IMF  $B_Z$  is positive (74%);
4. there exists a noticeable annual North-South asymmetry that, on the base of the present data, may be connected to a long-term external cause (e.g. the IMF variability in the inner heliosphere);
5. the analysis of the subset of quasi-full disk images shows that the Double Peak emission patterns are typically aligned in longitude, without any appreciable longitudinal shift possibly produced by a strong IMF  $B_Y \neq 0$ . It also shows that the Na emission is mostly located in the pre-noon sector (53%), which is roughly facing the local Parker's spiral direction, and close to the noon meridian (36%).